ORIGINAL PAPER

ANALYTICAL MODEL AND NUMERICAL FINITE ELEMENT MODEL FOR A SUBMERSIBLE SYNCHRONOUS HYDROGENERATOR

CONSTANTIN DUMITRU[1], FLORENTINA BUNEA[1,*], ADRIAN NEDELCU[1], NICOLAE TANASE[1], GHEORGHE MIHAI MIHAIESCU[1]

Manuscript received: 12.10.2022; Accepted paper: 21.12.2022;
Published online: 30.03.2023.

Abstract. *The main objective of the paper is to demonstrate the functionality and reliability of a hydrokinetic turbine system – a submersible electric generator, suitable for very low watercourses. To achieve this goal, it is necessary to design and build a prototype of a hydrokinetic turbine, coupled with an electric generator with excitation made with permanent magnets. This paper presents an analytical model and a finite element numerical model for estimating the electrical parameters of the generator (voltage, current, power, etc.). The two models were compared, and the results were extrapolated, in the analytical model, for several speed values.*

Keywords: *permanent magnet synchronous generator; finite element in time domain analyses; analytical model.*

1. INTRODUCTION

Permanent magnet synchronous generators (PMSGs) are widely used in wind and hydro energy conversion systems, especially for their high efficiency, stability, low rotational speed and the lack of additional DC excitation supply. Many researchers are interested in the designing and optimization of the PMSGs suitable for their specific applications [1-3].

This paper presents a submersible permanent magnet synchronous generator (PMSG) used in a hydrokinetic turbine system. Synchronous generators are especially suitable for island systems of the picohydro power plant type (with power less than 10 kW).

The proposed power system aims at practical use, to provide green energy, being able to be installed in a nearby watercourse. Thus, the aim of the paper is to develop a prototype that can obtain electricity from watercourses in places where the hydraulic head is very low. In the context of an accelerated dynamic of the use of renewable resources, increasing energy production and reducing the impact on the environment is an up-to-day subject.

The factors influencing the conversion efficiency are mainly related to the rotor and electric generator type. The water velocity is particularly important because a doubling of it causes an approximately 8-fold increase in energy density. Currently, there are various conceptual solutions for hydrokinetic turbines, but their efficiency is considerably low compared with conventional hydroelectric plants [4]. Therefore, the problem of increasing the conversion efficiency of kinetic energy still remains a current topic, under the attention of

[1] INCDIE ICPE – CA, Department of Renewable Energy Sources and Energy Efficiency, 030138 Bucharest, Romania. E-mail: constantin.dumitru@icpe-ca.ro; adrian.nedelcu@icpe-ca.ro; nicolae.tanase@icpe-ca.ro.
Corresponding author: florentina.bunea@icpe-ca.ro,

researchers in order to increase their physical and economic feasibility [5-6]. Classic solutions are constantly improved and in parallel, new solutions are developed worldwide that offer higher yields [7-9]. In [10] an experimental model of the hydrokinetic turbine is presented and many flow velocities and rotational speeds were investigated to characterize the turbine efficiency. These kinds of turbines are simple to install and operate and the maintenance costs are convenient, but predicting turbine performance is essential for large-scale implementation [11, 12], thus, many different prediction models are developed.

2. THE 3D CAD MODEL OF THE HYDROGENERATOR

To comply with the technical conditions of operation of the hydro aggregate with the kinetic turbine, immersion in the direction of the water stream, the actual construction considers: the rotor (1), the casing (2), the shields (3), (4) and shaft (5) are sized according to the mechanical stresses at the level of the hydro aggregate assembly, Fig. 1; the sealing of the static parts is done with O-rings at the level of the shields - the casing, Fig. 2a; the sealing at the level of the traction-motion shaft is made with a mechanical sealing device from ROSEAL type EFS163 S045 U1U1S2 G5G1, having the following components: rubber bellows (1), pressing ring (2), spring (3), pressing ring (4), mobile ring (5), fixed ring (6), secondary sealing (7), Fig. 2b; the shaft bearing is made with ball bearings. The anti-thrust bearing is of the radial-axial type with double-row balls to absorb the axial loads generated by the rotating turbine.

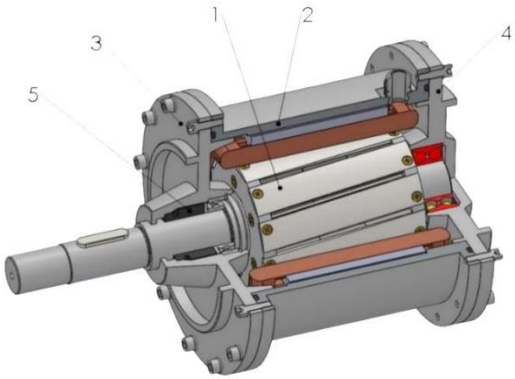

Figure 1. Generator assembly, 3D CAD model.

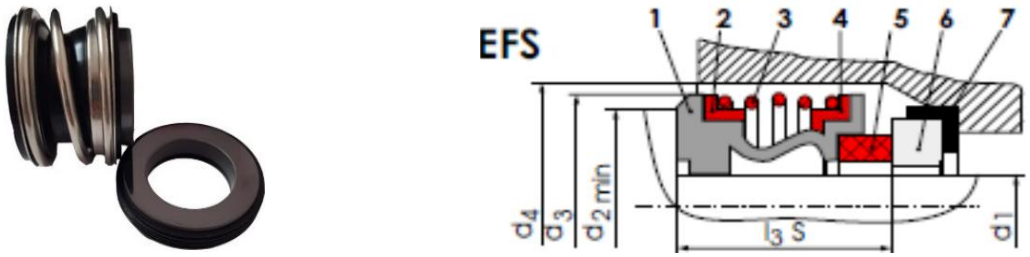

a) **b)**

Figure 2. Generator mechanical seal device.

The rotor subassembly, shown in Figs. 3 and 4, is made of the following components:

1. rotor shaft;
2. safety ring for axial fixation of the 12-pole rotor core on the shaft;
3. side flange for fixing the magnetic core and the 12 polar soles;
4. magnetic core rotor with 12 poles;
5. permanent magnets DfES, 36 pcs.;
6. polar sole.

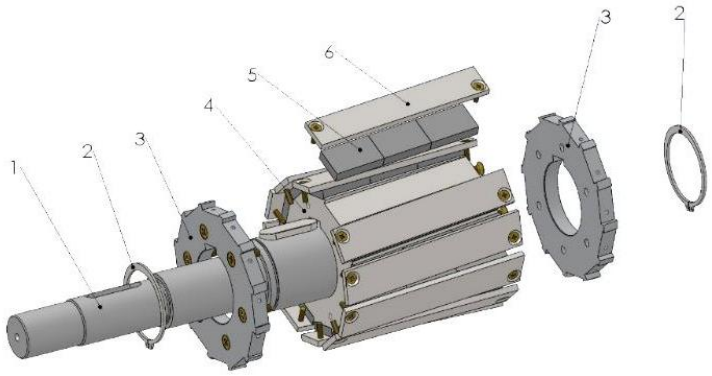

Figure 3. Three-phase synchronous generator mounted rotor subassembly, exploded view 3D CAD model.

Figure 4. Rotor subassembly.

3. DESCRIPTION OF THE ANALYTICAL MODEL

In Fig. 5 is presented the block diagram of the electrical circuit of the assembly, having the following elements: hydrokinetic turbine (1); the three-phase synchronous generator (2); rectifier bridge (3); DC voltage variator (4) to provide an imposed voltage for charging the battery bank (5); the single-phase or three-phase inverter (6) to provide alternating voltage to the consumer (7).

The estimated maximum power is 1100 W. The reference speed range is 150-300 rpm. In order to increase the efficiency of the electrical circuit of the assembly, the generator has a relatively high electrical voltage output.

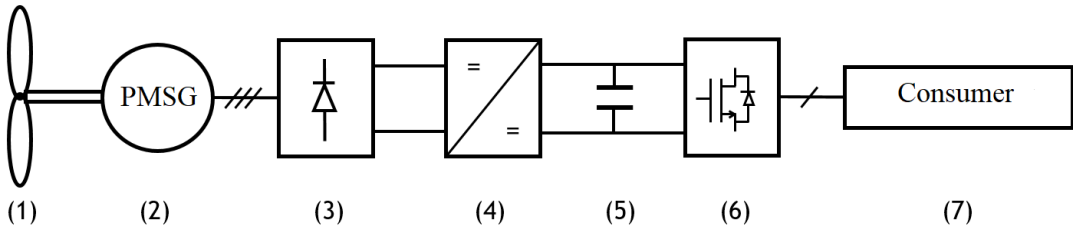

Figure 5. Block diagram of the electrical circuit of the assembly.

The analytical model of the PMSG was implemented in MATLAB, having as input parameters rotational speed (n) and current density (J1), and as outputs the operating parameters, e.g. line voltage (UL), phase current (I), voltage drop (ΔU), electric power (P), etc. The program generates several characteristics of output parameters at different operational conditions, as shown in Figs. 6 and 7. The red line marks the imposed current density limit. The analytical model does not consider the magnetic saturation effect of the sheet, thus the U-I characteristic is linear.

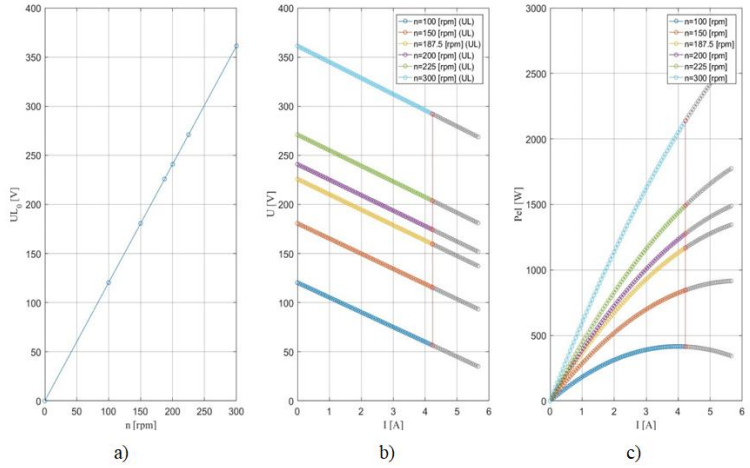

Figure 6. a) No-load operation characteristic; b) Load operation characteristic; c) Power characteristic as a function of current.

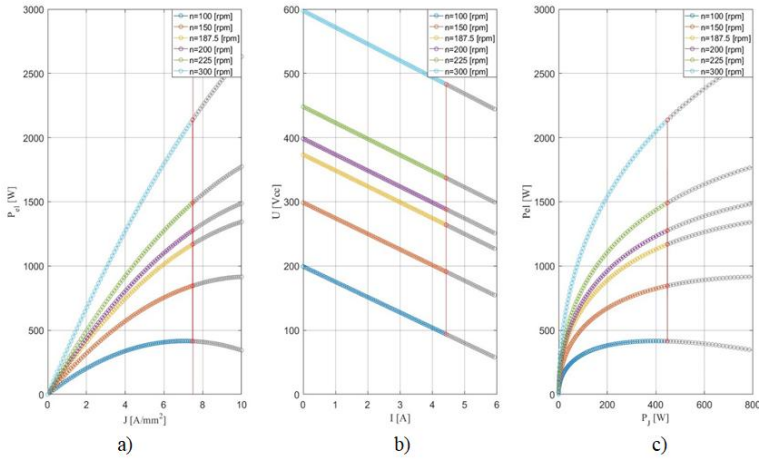

Figure 7. a) Power characteristic depending on the current density; b) Load operation characteristic (after rectification); c) Power curve depending on Joule losses.

4. DESCRIPTION OF THE NUMERICAL FINITE ELEMENT MODEL

Based on previous research on a submersible electrical generator with a similar topology of the rotor, it was determined that by reducing the 3D geometry to 2D planar (mid-plane, not taking into account the effect of rotor skewing) the error of the numerical model will not exceed 6%. The error being less than expected for this kind of numerical model, the design of the current generator was carried out with the help of a simplified 2D numerical finite element model, with a considerable economy of computational resources.

The finite element numerical model was made in Altair FLUX 2D software. The value of the remnant magnetic flux density of the magnets used is considered Br=1.1 [T]. In the numerical model, the non-linear B-H characteristic of the stator sheet FLU_M600_65A was used.

In Fig. 8 is presented the simplified geometry of the generator, having the following elements: casing (1), stator sheet (2), stator winding (3), permanent magnets (4), polar sole (5), rotor magnetic core (6), shaft (7). The permanent magnets (4) are represented with two colors, red and blue, to highlight their alternative placement. In Fig. 9 is presented the mesh

associated with the geometry and in Fig. 10 is shown the electrical circuit associated with the geometry.

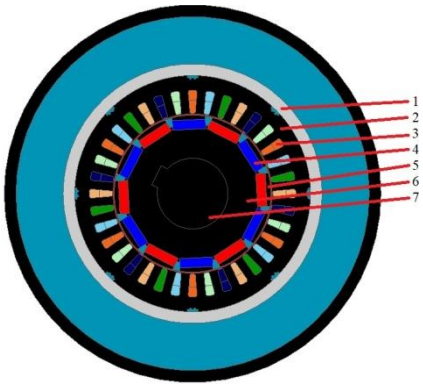

Figure 8. Simplified geometry of the generator.

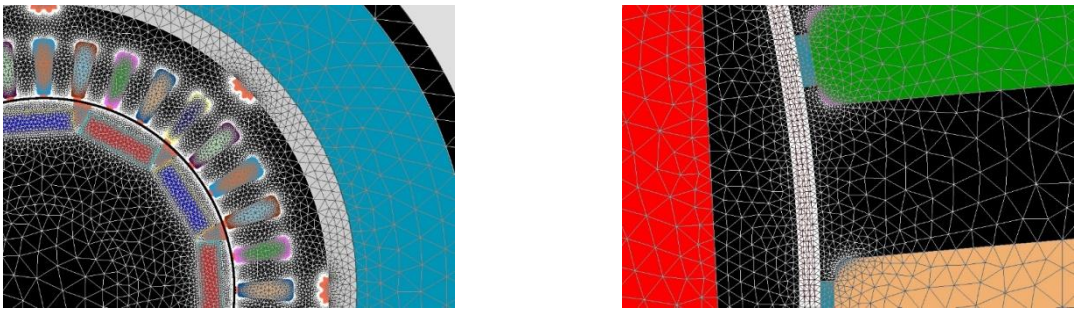

Figure 9. The mesh associated with the geometry.

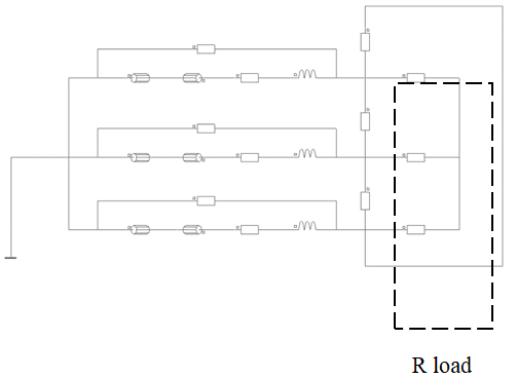

Figure 10. The electrical circuit associated with the geometry.

4.1. NO LOAD OPERATION OF THE PMSG

The worst case in the operation of the generator is represented by the speed of 150 rpm where the losses in GS are significant. Thus, three operating point models of GS were compared.

Time dependence and harmonics of the line voltage at no load operation of PMSG at 150 rpm are presented in Fig. 11. Also, the computed parameters are shown in Table 1. Due to the skewing effect of the rotor of the experimental model, the harmonics will be reduced.

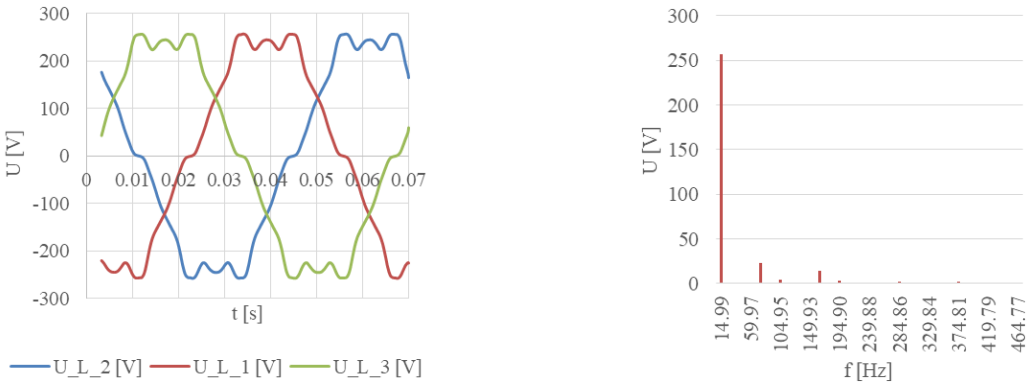

Figure 11. Time dependence and harmonics of the line voltage.

Table 1. Computed parameters for no load operation of PMSG.

Model	***n* [rpm]**	***f* [Hz]**	***R load* [Ω]**	***U_L0* [V]**
Analytical	150	15	1e7	180.653
Numerical	150	14.99	1e7	182.794
Relative error [%]	0	-0.05	0	1.171

For the no-load operation of the PMSG, the relative error of the line voltages has the lowest value, compared with the load operation. The line voltage was estimated using the equation (1), [13]:

$$U_{L0} = \sqrt{3} \cdot (4 \cdot k_B \cdot f \cdot k_{w1} \cdot w_1 \cdot \Phi)/k_E \tag{1}$$

4.2. LOAD OPERATION OF THE PMSG

In Fig. 12 is shown the pseudo-colored map of the magnetic flux density and lines of the magnetic field for load operation at the speed of 150 rpm, where it is noticeable that the maximum value of the magnetic flux density is found at the tip of the stator teeth and in the edges of the polar soles.

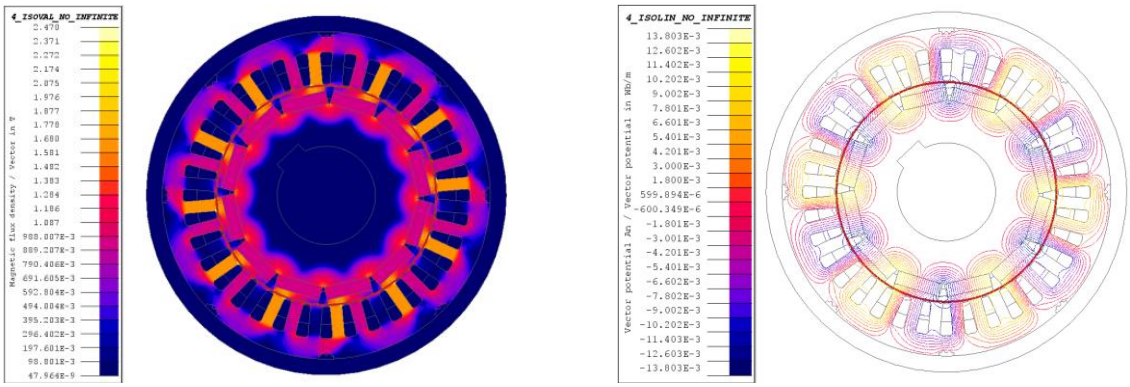

Figure 12. Map of the magnetic flux density and lines of the magnetic field for load operation.

Time dependence and harmonics of the line voltage and current at load operation of PMSG at 150 rpm are presented in Figs. 13 and 14. Also, the computed parameters are shown in Table 2.

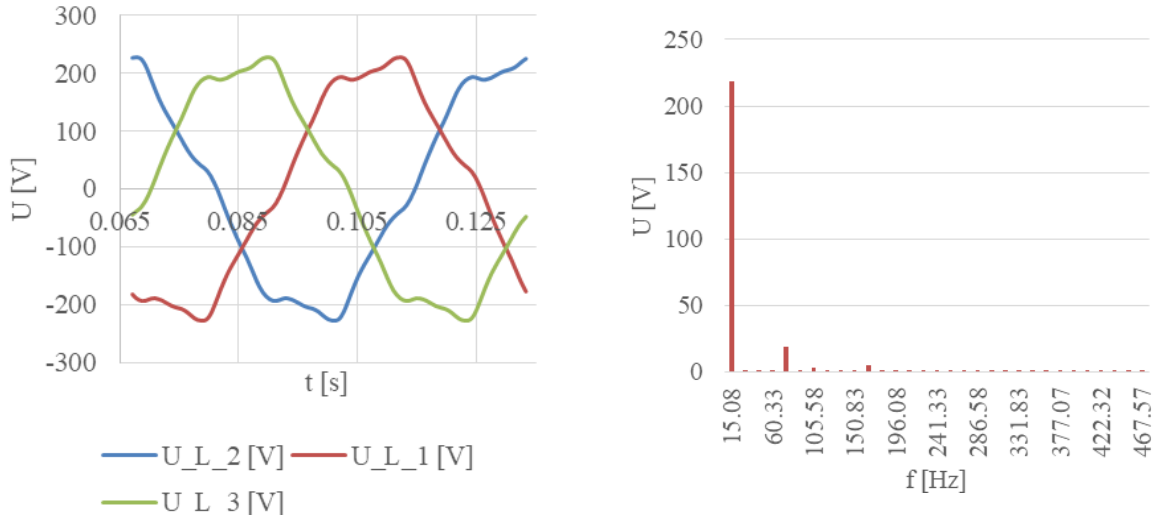

Figure 13. Time dependence and harmonics of the line voltage.

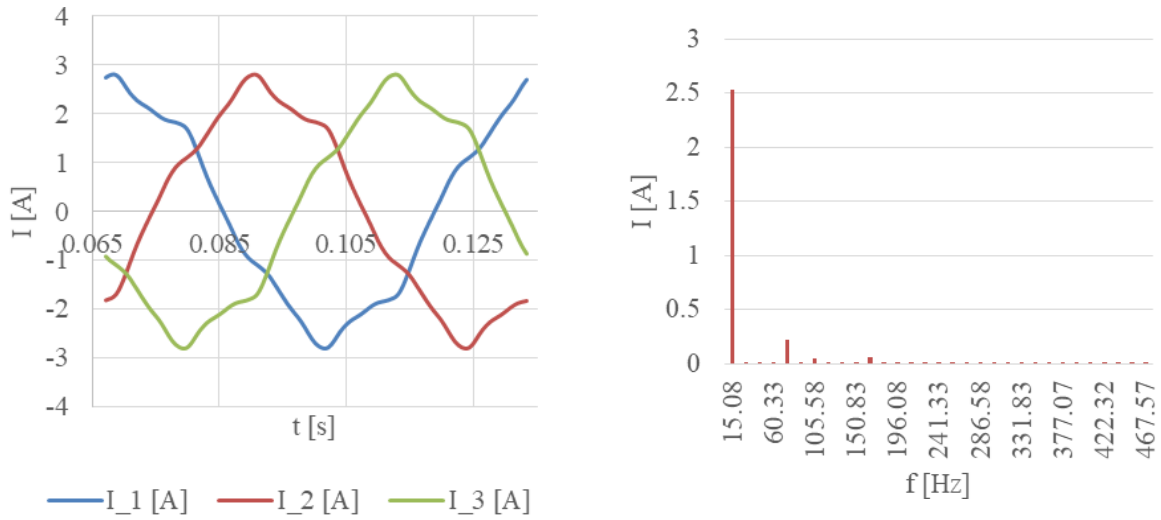

Figure 14. Time dependence and harmonics of the current

Table 2. Computed parameters for load operation of PMSG.

	***n* [rpm]**	***f* [Hz]**	***R load* [Ω]**	***UL* [V]**	***Uph* [V]**	***Iph* [A]**
Analytical model	150	15	48.705	152.689	87.834	1.803
Numerical model	150	15.083	49.7175	155.298	89.662	1.80342
Relative error [%]	0	0.55	2.03671	1.68	2.0384	0.0011
	***Pel* [W]**	**Δ*U* [%]**	**cos φ**	***T* [Nm]**	***Pmech***	***J1***
Analytical model	475.2	15.47916	1	-	-	3.189
Numerical model	485.092	15.04174	1	36.0815	566.767	3.189
Relative error [%]	2.039	2.908	0	-	-	0.00146

Continued

Casing losses [W]	0.000366
Losses in magnets [W]	0.021912
Losses in polar soles [W]	0.567537
Joule losses [W]	81.4543
Friction losses [W]	31.41593
Losses in the rotor core [W]	0.025578
Losses in the stator core [W]	9.135872
Efficiency [%]	79.82

The efficiency was estimated using equation (2), [13], where *Pel* is the electrical power and *ΣP* is the sum of all losses in PMSG.

$$\eta[\%] = \frac{Pel}{Pel + \sum P} \cdot 100 \tag{2}$$

4.3. MAXIMUM LOAD OPERATION OF THE PMSG

The maximum load represents the load at which the generator can operate only for a short period of time without damaging the insulation of the conductors, taking into account that the PMSG is submersible. In Table 3 are shown the computed parameters.

Table 3. Computed parameters for maximum load operation of PMSG.

	***n* [rpm]**	***f* [Hz]**	***R load* [Ω]**	***UL* [V]**	***Uph* [V]**	***Iph* [A]**
Analytical model	150	15	17.4278	120.0053	69.2851	3.9755
Numerical model	150	15.083	17.4278	119.959	69.2581	3.974
Relative error [%]	0	0.55	0	-0.0389	-0.03891	-0.03764
	***Pel* [W]**	**Δ*U* [%]**	**cos φ**	***T* [Nm]**	***Pmech***	***J1***
Analytical model	826.3287	33.57123	1	-	-	7.0303
Numerical model	825.697	34.37484	1	77.7533	1221.35	7.02758
Relative error [%]	-0.07657	2.337796	0	-	-	-0.0387
Casing losses [W]					3.07E-04	
Losses in magnets [W]					0.047786	
Losses in polar soles [W]					0.10772	
Joule losses [W]					395.528	
Friction losses [W]					31.41593	
Losses in the rotor core [W]					0.025578	
Losses in the stator core [W]					9.135	
Efficiency [%]					65.43	

5. CONCLUSION

A new dedicated electric generator has been designed for a direct drive MICROHIDRO application. An analytical model and a numerical model using finite elements were developed to estimate the electrical parameters of the generator's operation (voltage, current, power, etc.). The models can be used to optimize the generator design for a specific hydro turbine – a necessary step in the design of direct drive configurations. The analytical model, although lacking precision, is considerably faster than finite element models. Using a combination of these two types of models offers the advantage of reduced computational time and still retaining adequate precision.

Acknowledgment: *This paper was carried out under the subsidiary contract126-D4/2020, Hydrokinetic turbine suitable for natural and artificial watercourses, with a small head, MICROHIDRO, Transenerg, POC 2014-2020, P_40_432/105567, Contract no. 126/16.09.2016. The work was also supported by the Romanian Ministry of Education, Research and Digitalization, project number 25PFE/30.12.2021.*

REFERENCES

[1] Ghita, C., Nedelcu, S., Trifu, I., Tudorache, T., *UPB Scientific Bulletin*, **75**(1), 241, 2013.
[2] Popescu, M., Cistelecan, M., Melcescu, L., Covrig, M., *Proceeding of 2007 International Conference on Clean Electrical Power*, 9728140, 2007.
[3] Tudorache, T., Melcescu, L., Popescu, M., Cistelecan, M., *Renewable Energy and Power Quality Journal*, **1**(6), 692, 2008.
[4] Cardona-Mancilla, C., Sierra-Del Rio, J., Hincapié-Zuluaga, D., Chica, E., *International Journal of Renewable Energy Research*, **8** (4), 1833, 2018.
[5] Hasmatuchi, V., Alligné, S., Kueny, J. L., Munch, C., Hydraulic performance of a new isokinetic turbine for rivers and artificial channels, *E-proceedings of the 36th IAHR World Congress*, **1**, 2015.
[6] Gaden, D. L. F., Bibeau, E. L., *Renew.Energy*, **35** (6), 1152, 2010.
[7] Javaherchi, T., Stelzenmuller, N., Aliseda, A., *J. Renew. Sustain. Energy*, **9**, 044504, 2017.
[8] Nedelcu, A., Bunea, F, Danca, P.A., Chihaia, R.A., Babutanu, C.A., Marin, D., Ciocan, G.D., Experimental research on a hydrokinetic turbine model, *IOP Conference Series: Earth and Environmental Science*, **664**, 012061, 2021.
[9] Danca, P. A., Bunea, F., Nicolaie, S., Nedelcu, A., Tanase, N., Babutanu, C. A., Study of Hydrokinetic Turbine Shrouds, *10th International Conference on Energy and Environment*, 1-5, 2021. doi.org/10.1109/CIEM52821.2021.9614929.
[10] Chihaia, R.A., Bunea, F., Oprina, G., El-Leathey, L.A., *Power Prediction Method Applicable to Horizontal Axis Hydrokinetic Turbines, Proceeding of IEEE 2017 International Conference on Energy and Environment*, 17412292, 2017. doi.org/10.1109/CIEM.2017.8120825.

[11] Lawson, M., Li, Y., Sale, D., Development and verification of a computational fluid dynamics model of a horizontal-axis tidal current turbine, *Proceeding of the 30th International Conference on Ocean, Offshore and Arctic Engineering*, Paper No. OMAE2011-49863, 711, 2011. https://doi.org/10.1115/OMAE2011-49863.
[12] Nachtane, M., Tarfaoui, M., Goda, I., Rouway, M., *Renewable Energy*, **157**, 1274, 2020.
[13] Cioc I., Nica C., *Proiectarea mașinilor electrice*, Didactica si Pedagogica Publishing House, Bucharest, pp. 299&920, 1994.